

## Effect of Korteweg Stress in Miscible Liquid Two-Layer Flow in a Microfluidic Device

Sugii, Y.\*<sup>1</sup>, Okamoto, K.\*<sup>1</sup>, Hibara, A.\*<sup>2</sup>, Tokeshi, M.\*<sup>3</sup> and Kitamori, T.\*<sup>2</sup>

\*1 Department of Quantum Engineering and Systems Science, University of Tokyo, 7-3-1, Hongo, Bunkyo-ku, Tokyo 113-8656, Japan. E-mail: sugii@q.t.u-tokyo.ac.jp

\*2 Department of Applied Chemistry, University of Tokyo, 7-3-1, Hongo, Bunkyo-ku, Tokyo 113-8656, Japan.

\*3 Integrated Chemistry Project, Kanagawa Academy of Science and Technology, 3-2-1, Sakado, Takatsu-ku, Kawasaki-shi, Kanagawa 213-0012, Japan.

Received 19 August 2004  
Revised 6 December 2004

**Abstract** : Miscible liquid two-layer flow in a Y-shaped microfluidic device, which consists of microchannels with 120  $\mu\text{m}$  in width and 35  $\mu\text{m}$  in depth, is investigated by particle image velocimetry (PIV) to clarify the flow characteristics at fluid interfaces. The obtained velocities with a spatial resolution of  $5.9 \times 1.5 \mu\text{m}^2$  around the interface between water and ethanol indicate an imbalance in shear stress at interface. The reason of the imbalance is to be the Korteweg stress generated by interfacial tension gradient due to a concentration gradient by diffusion in a miscible two-layer flow. The stress may cause an interfacial instability and destroy a uniform mixing in two flowing fluids in the case of large concentration gradient.

**Keywords** : Korteweg stress, Continuous flow chemical processing, Interfacial tension, Miscible liquid flow, Micro PIV.

### 1. Introduction

Micro total analysis systems ( $\mu\text{TASs}$ ), or labs-on-a-chip, are microfluidic devices developed for chemical and biological analysis (Berug and Berg, 1995, Weigl and Yager, 1999). As these microfluidic devices have been miniaturized to sizes on the order of 100  $\mu\text{m}$ , several interesting features have become apparent. In particular, the flow characteristic on a microscopic scale differ from those predicted by the models accepted for macroscopic flow due to microscopic factors that can be neglected on larger scales (Ho and Tai, 1998). At micro scales, surface forces dominate the flow because of the larger surface area-to-volume ratio, resulting in drastic reduction in inertia and a substantial increase in the frequency response. The specifics of this behavior become important in applications such as capillary electrophoretic separation in fabricated microchannels on a microchip, which is a device with enormous analytical potential for miniaturized separation.

Continuous-flow chemical processing (CFCP) based on microunits such as mixers and reactors, complicated chemical systems has been proposed (Tokeshi et al., 2002). Mixing or chemical reactions, in which two or more fluids flow in parallel in microchannels, can be generated continuously because of the transfer of molecules or ions from one fluid to others by diffusion through interfaces. Significant extraction of Cobalt-2-nitroso-5-dimethylaminophenol, Ni-dimethylglyoxime methyl red

and so on has been demonstrated through a stable interfaces with immiscible two fluids such as an aqueous and organic and with miscible two fluids such as an aqueous and alcohol (Sato et al., 1999). Mixer or diffusion diluter with miscible two fluids, in which two liquids combine into a single stream and mix by diffusion as the liquid progress down the channel, has been also developed (Holden et al. 2003). Interfacial instability in two flowing fluids often occurs such as Kelvin - Helmholtz instability or Rayleigh - Taylor instability. The instability often destroys stable interface in the case of immiscible or miscible two liquids flow. In order to investigate interfacial phenomena, a quasi-elastic laser scattering method has been applied to measurement capillary wave, whose beat frequency is related to interfacial tension, in miscible and immiscible liquids (Hibara et al., 2003). The results indicated that the evidence of an interfacial tension of miscible liquids, which generates capillary wave at the interface. Therefore, it is important to investigate the flow characteristics on these microscopic scales to achieve a stable interface.

In the present study, micro-PIV technique was applied to the analysis of miscible liquid two-layer flow, side-by-side flow, in a micro fluidic device to clarify the flow characteristics at an interface. The momentum balance between water - ethanol flow around an interface was investigated using measured velocity distributions.

## 2. Experimental Method

The microchip was fabricated on Pyrex substrates using standard photolithographic and wet chemical etching techniques and thin glass plate was covered on the top (Hibara et al., 2001). Figure 1 shows a schematic illustration of the microchip. The microchip was a Y-junction between two inlets and one outlet, fabricated as microchannels of 120  $\mu\text{m}$  in width and 35  $\mu\text{m}$  in depth at the deepest point (semi-circular cross-section) shown in Fig. 1(c). Two fluid systems were examined: ion-exchanged water only, and ion-exchanged water and ethanol (80.0 vol%). The two liquids were introduced into the inlets of the microchip at a constant flow rate using two independent syringe pumps of 250  $\mu\text{L}$  capacity. The flow rates at the inlet for the water - water case were set to 500  $\mu\text{L}/\text{h}$ , and for water - ethanol case were set to 500  $\mu\text{L}/\text{h}$  water and 400  $\mu\text{L}/\text{h}$  ethanol. The ethanol flow rate was set such that the interface at the Y-junction would remain at the midpoint in the downstream channel. The refractive indexes of water and ethanol are 1.33 and 1.36, and the densities are 1.0 and 0.79  $\text{g}/\text{cm}^3$  at 10  $^\circ\text{C}$ , respectively. Ethanol is readily soluble in water, and has a diffusion coefficient  $D = 1.0 \times 10^{-6} \text{ cm}^2/\text{s}$ .

Figure 2 shows a schematic of experimental set up of micro PIV system. Micro PIV technique, which is a quantitative method for measuring velocity fields with micro resolution instantaneously in experimental fluid mechanics systems (Santiago et al., 1998), is useful for investigation of flow in micro fluidic devices (Sugii and Okamoto, 2004, Kim and Kihm, 2004). Fluorescent particles with diameter of 1  $\mu\text{m}$  and density 1.05  $\text{g}/\text{cm}^3$  were dispersed in the water and ethanol for PIV. The fluorescent particles absorb green light (peak wavelength 535 nm) and emit orange light (575 nm). The observation region was illuminated with a double-pulsed Nd:YAG laser (532 nm) captured through a microscope equipped with an oil-immersion objective lens ( $M = 60$ ,  $\text{NA} = 1.25$ ). The particle images were recorded using high-sensitivity charge-coupled device (CCD) camera equipped with an optical filter (low-pass: 550 nm) such that only the fluorescence was imaged. The images were obtained as 12-bit grayscale images of 1280 x 1024 pixels in size. Images were recorded in pairs 125 ms apart, and the system was capable of recording a total of 164 image pairs. PIV analysis was conducted by synchronizing the double pulses of the laser with the shutter of the camera using a pulse generator.

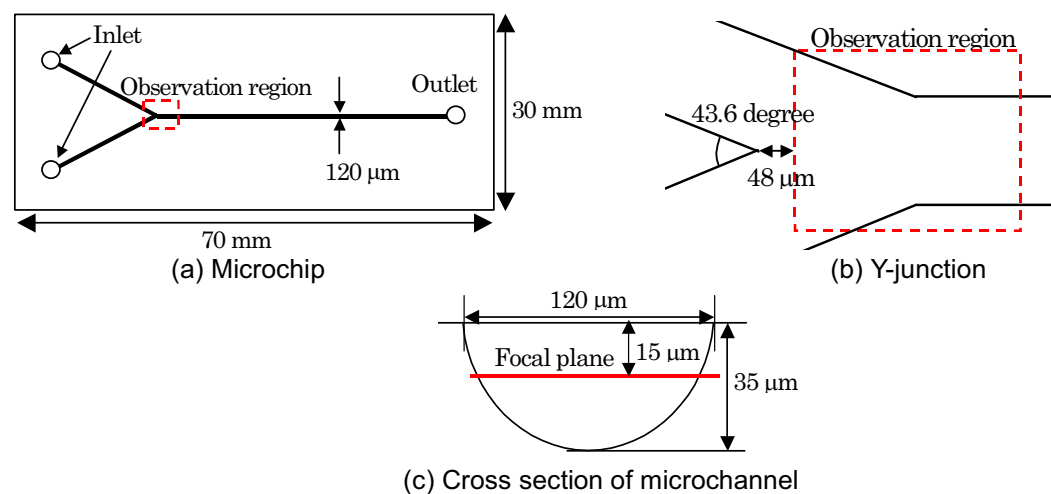


Fig. 1. Schematic of Y-junction microchip.

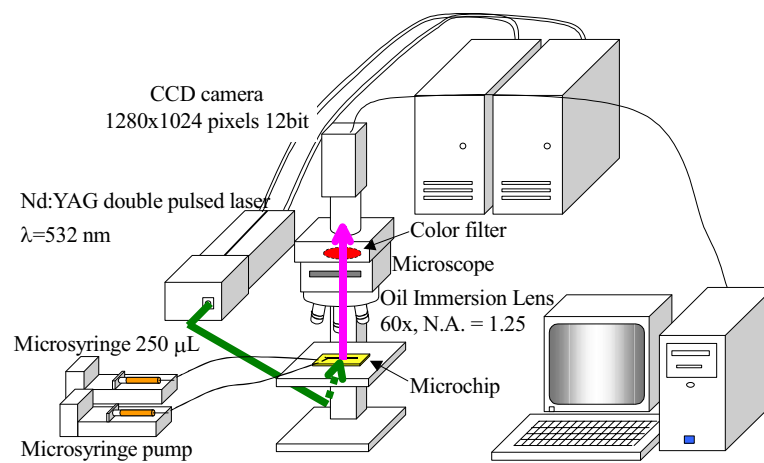


Fig. 2. Schematic of Micro PIV system.

### 3. Results

Figure 3 shows a plain-light image of the water - ethanol experiment under illumination by a halogen light. The focal plane was set to 15  $\mu\text{m}$  depth from top shown in Fig. 1(c). The difference of the focal plane between the two fluids caused by different refractive indexes was estimated as 0.25  $\mu\text{m}$ . As the inner walls were tilted slightly in the depth direction because of the semi-circular profile, the walls are clearly observed as black bands. The observation region was 231 x 184  $\mu\text{m}^2$  in size immediately downstream of the junction such that the length between the confluence point and the left edge of the image was 48  $\mu\text{m}$ , and each pixel in the image represents a 0.18 x 0.18  $\mu\text{m}^2$  area. Water was introduced into the left inlet, and ethanol was introduced into the right inlet. The interface between water and ethanol can be clearly seen in the center of the image at about  $y = 90 \mu\text{m}$  due to refraction caused by the difference in refractive indexes of the two liquids. Although the interface was slightly curved, it was steady and stable in all experiments due to the choice of flow rates.

A fluorescent particle image under illumination by the Nd:YAG double pulsed laser is shown in Fig. 4. Particles appear as bright points of light. Background noise is due to out-of-focus particles and light scattering by the channel walls. One particle was observed as a 7-8 pixel area of brightness in

the image. Applying the highly accurate PIV technique (Sugii et al., 2000) to the images, the time-averaged velocity distributions of 164 maps in case of (a) water - water at flow rate 500  $\mu\text{L}/\text{h}$  and (b) water - ethanol at 500  $\mu\text{L}/\text{h}$  water and 400  $\mu\text{L}/\text{h}$  ethanol were obtained shown in Fig. 5. Color in the figure represents a velocity magnitude. Background noise due to out-of-focus particles was removed by subtracting a background intensity calculated from the series of images. An interrogation window of  $65 \times 17$  pixels was taken with 50% overlap, corresponding to a spatial resolution of  $5.9 \times 1.5 \mu\text{m}^2$ . Eighty velocity values were obtained along the capillary diameter for each channel. The flow in each channel with 120  $\mu\text{m}$  width at the upstream of the junction was fully developed. Since channel width decreased half size after the junction, the flow was accelerated and then fully developed again. Velocity vectors out of flow region were zero because of eliminating background noise. The velocity vectors very close to the wall were measured and it was found that the wall-normal component of the velocity vectors was close to zero. Since the variation of time series of velocity distribution, which was less than 5 % of the averaged velocity, was small enough, pulsation of flow due to syringe pump was small enough. In the case of (b) water - ethanol, the flow in each channel at the upstream of the junction was also fully developed. However, difference between velocities of inlet channels was clearly observed due to different flow rate. After junction, the flow was accelerated.

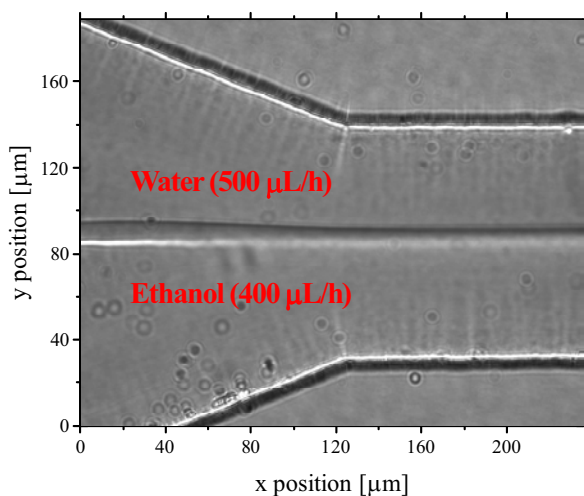


Fig. 3. Plain-light image of interface between water and ethanol.

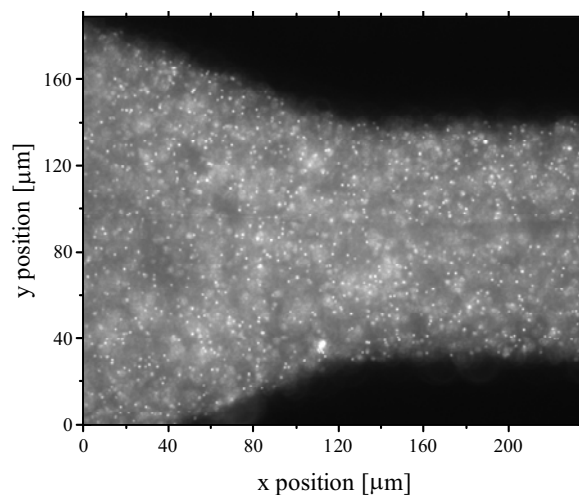
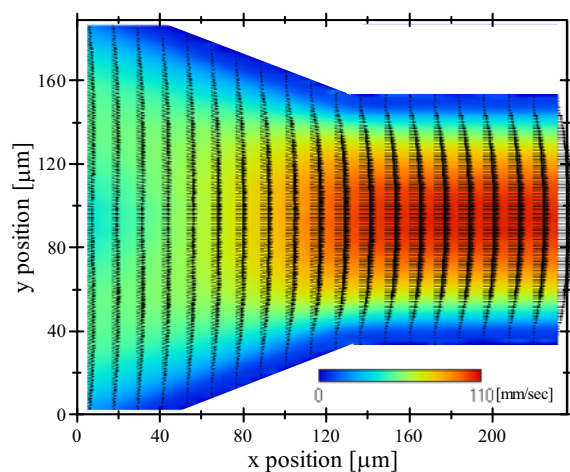
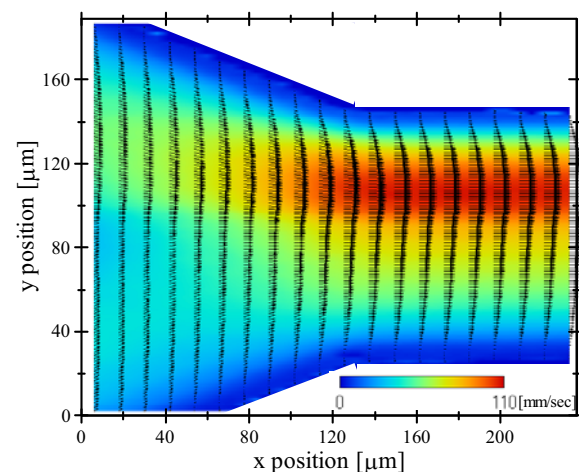


Fig. 4. Fluorescent particle images of Y-junction under pulsed Nd:YAG laser light.



(a) Water - water



(b) Water - ethanol

Fig. 5. Time-averaged velocity distributions.

In order to investigate the dynamics around the interface in detail, time-averaged axial velocity profiles in four cross-sections are shown in Fig. 6. In the water - water experiment, all profiles were symmetric. At the most upstream section,  $x = 5.9 \mu\text{m}$ , two peaks of almost the same velocities were observed at the center of each channel. The flow in each channel upstream of the junction was fully developed. Since the effective channel width reduced by half at the junction, the flow was accelerated at  $x = 59.0$  and  $112 \mu\text{m}$ , and then became fully developed again at  $x = 218 \mu\text{m}$  resulting in a single peak profile. Velocity profiles at the downstream region beyond  $x = 150 \mu\text{m}$  have almost same values. At the most downstream section,  $x = 218 \mu\text{m}$ , the velocity reached a maximum of about  $107 \text{ mm/s}$  near the center, tapering off to zero at the wall. This profile corresponds closely to the theoretical Stokes profile except near wall region shown in Fig. 5(a). Conversely, in the water - ethanol experiment, all profiles were asymmetric. At the most upstream section,  $x = 5.9 \mu\text{m}$ , the channel flow was fully developed, with different peak velocities in each of the two inlet channels. The flow accelerated at  $x = 59.0$  and  $112 \mu\text{m}$ , and then became fully developed again at  $x = 218 \mu\text{m}$ . At the most downstream section,  $x = 218 \mu\text{m}$ , the velocity peaked at around  $y = 110 \mu\text{m}$ , in the water region. Velocity profiles beyond  $x = 150 \mu\text{m}$  also have same values.

Figure 7 shows the velocity profile and shear rate at  $x = 218 \mu\text{m}$ . The shear rate was estimated using difference method. In each region, shear rates calculated using the difference approximation were linear. An inflection of velocity and discontinuity of shear rate were observed around the interface at  $y = 90 \mu\text{m}$ , indicating an imbalance of viscous force. Shear rates of ethanol and water are  $1.0 - 0.4$  and  $2.0 - 3.0 \times 10^3 \text{ 1/s}$ , the range estimated by the values from the graph or extrapolated values from the linear fits to the data. Therefore, shear stresses in ethanol and water are  $1.5 - 0.6$  and  $2.6 - 3.9 \text{ N/m}^2$ . Thus, the difference of shear stress is more than  $1.1 \text{ N/m}^2$ .

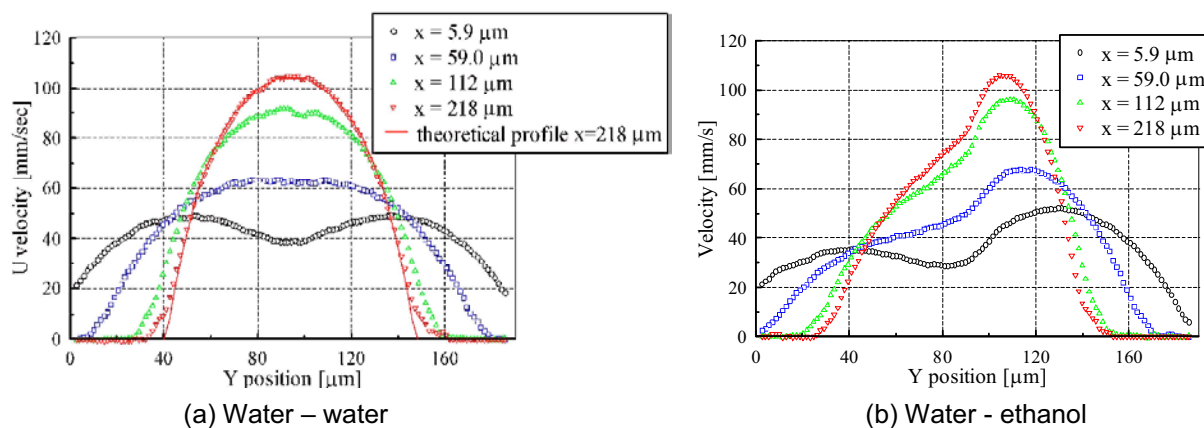


Fig. 6. Time-averaged axial velocity profiles.

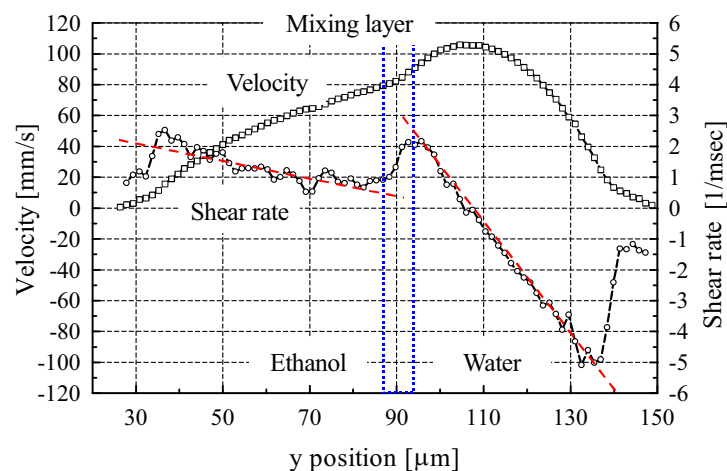


Fig. 7. Time-averaged axial velocity profile and shear rate.

## 4. Discussion

The reason for the imbalance of the shear stress at the interface is mainly considered as the existence of the Korteweg stress (Korteweg, 1901), which mimics surface tension in regions where the gradients are large, induced by gradients of density and concentration in miscible liquids. Mathematical formation of the stress in two incompressible miscible liquids was proposed (Joseph et al., 1996). It was reported that convection for miscible liquids under a micro-gravity condition can occur, which is analogous to surface tension induced convection by numerical simulation based on Korteweg stress (Volpert et al., 2002). The stress  $\mathbf{T}$  in two-dimensional flow was expressed as,

$$T_{11} = k \left( \frac{\partial C}{\partial y} \right)^2, T_{12} = T_{21} = -k \frac{\partial C}{\partial x} \frac{\partial C}{\partial y}, T_{22} = k \left( \frac{\partial C}{\partial x} \right)^2 \quad (1)$$

where  $C$  is the mass fraction of liquid,  $k$  is a system-specific parameter.

The governing equations in incompressible miscible liquids were represented as,

$$\frac{\partial C}{\partial t} + (\mathbf{v} \cdot \nabla) C = D \nabla^2 C \quad (2)$$

$$\frac{\partial \mathbf{v}}{\partial t} + (\mathbf{v} \cdot \nabla) \mathbf{v} = -\frac{1}{\rho} \nabla p + \nu \nabla^2 \mathbf{v} + \frac{1}{\rho} \nabla \cdot \mathbf{T} \quad (3)$$

$$\nabla \cdot \mathbf{v} = 0 \quad (4)$$

where  $D$  is the diffusion coefficient,  $\mathbf{v}$  is the velocity,  $p$  is pressure,  $\nu$  is the kinematic viscosity, and  $\rho$  is the density.

The viscosity  $\nu$  and the density  $\rho$  depend upon the concentration  $C$ . Here, the balance between the shear stress and the Korteweg stress was considered. Since Reynolds number was significantly low about 1.0, and flow was steady and fully developed, the balance equation of the gradients of stresses can be introduced from Eq. (3) as

$$0 = \rho \nu \frac{\partial \dot{\gamma}}{\partial y} + k \frac{\partial}{\partial x} \left( \frac{\partial C}{\partial y} \right)^2 \quad (5)$$

where  $\dot{\gamma}$  is shear rate.

The gradient of the shear stress at  $x = 218 \mu\text{m}$  in Fig. 7 was in the range from  $0.6 \times 10^6$  to  $2.0 \times 10^6 \text{ N/m}^3$  at the first term of right hand in Eq. (5) in the mixing layer because of the varying viscosity. Viscosity increases sharply from 1.3 cP at pure water to a maximum of 4.2 cP at an ethanol concentration of around 40 vol% and then decreases to 1.5 cP at pure ethanol. Estimating the concentration distribution by Eq. (2) using measured velocity distribution numerically, the width of the mixing layer was  $10 \mu\text{m}$  and the diffusion angle was 0.17 degree approximately. Assuming that the concentration gradient in  $y$ -direction was linearly, the gradient of the Korteweg stress at the second term of the right hand side of Eq. (5) in the stream direction was approximately in the range of  $-0.84 \times 10^6$  to  $-1.1 \times 10^6 \text{ N/m}^3$ . The shear stress and surface tension gradient generated force, called as the Korteweg stress, were balanced at the interface of miscible two-layer flow. The phenomena were similar to Marangoni effect, which is caused by an interfacial tension gradient caused by temperature gradient. The Marangoni effect drives fluid toward the region of largest surface tension when there is a difference in surface tension between two points on a surface (Scriven and Sternling 1964). Surface tension of the mixture decreases with increasing ethanol concentration from 73.4 at pure water to 22.6 dyn/cm at pure ethanol and the gradient of surface tension is sudden around 0 - 10 % ethanol concentration and that is gently over 10 %. This means that interfacial tension of ethanol in upstream region was larger than that in down stream region, resulting in a stress generated toward the region of larger surface tension from the region of smaller tension.

## 5. Conclusion

The flow characteristics at an interface between water and ethanol in a Y-junction microchip were investigated using a micro-PIV technique. Velocity distributions with a spatial resolution of  $5.9 \times 1.5 \mu\text{m}^2$  were obtained. A stable interface was achieved by applying different inlet flow rates of water and ethanol. The velocities around the interface between water and ethanol were skewed, indicating an imbalance of shear stress at the interface. The reason of the imbalance is to be stress, so called the Korteweg stress, generated by interfacial tension gradient due to a concentration gradient by diffusion in a miscible multi-layer system. The stress may play an important role in interfacial instability both of immiscible and miscible liquids with molecular transportation in microscopic flow. It is expected that a concentration gradient of molecule caused by molecular transportation through the interface of oil and water could be often occurred, resulting in the generation of the stress.

### *Acknowledgements*

We gratefully acknowledge discussions with Prof. H. Madarame, University of Tokyo. This work was partly supported by a Grant-in-Aid for Scientific Research (B) 15360092, from the Ministry of Education, Culture, Sports, Science and Technology, Japan.

### *References*

- Berug, A. and van den Berg, A. Eds., *Micro Total Analysis Systems*, (1995), Kluwer Academic Pub.
- Hibara, A., Nonaka, M., Tokeshi, M. and Kitamori, T., *Spectroscopic Analysis of Liquid / Liquid Interfaces in Multiphase Micro*, *J. Am. Chem. Soc.*, 125 (2003), 14954-14955.
- Hibara, A., Tokeshi, M., Uchiyama, K., Hisamoto, H. and Kitamori, T., *Integrated multilayer flow system on a microchip*, *Anal. Sci.*, 17 (2001), 89-93.
- Ho, C. M. and Tai, Y. C., *Micro-electro-mechanical-systems (MEMS) and fluid flows*, *Ann. Rev. Fluid Mech.*, 30 (1998), 579-612.
- Holden, M. A., Kumar, S., Castellana, E. T., Beskok, A. and Cremer, P. S., *Generating fixed concentration arrays in a microfluidic device*, *Sensors and Actuators B*, 92 (2003), 199-207.
- Joseph, D., Huang, A. and Hu, H., *Non-solenoidal velocity effects and Korteweg stress in simple mixture of incompressible liquids*, *Physica D*, 97 (1996), 104-125.
- Kim, M. J. and Kihm, K. D., *Microscopic PIV measurements for electro-osmotic flows in PDMS microchannels*, *J. Visualization*, 7-2 (2004), 111-118.
- Korteweg, D. J., *Sur la forme que prennent les équations du mouvements des fluides si l'on tient compte des forces capillaires causées par des variations de densité considérables mais connues et sur la théorie de la capillarité dans l'hypothèse d'une variation continue de la densité*, *Archives Néerlandaises des Sciences Exactes et Naturelles*, 6 (1901), 1-24.
- Santiago, J. G., Wereley, S. T., Meinhart, C. D., Beebe, D. J. and Adrian, R. J., *A particle image velocimetry system for microfluidics*, *Exp. Fluids*, 25 (1998), 316-319.
- Sato, K., Tokeshi, M., Kitamori, T. and Sawada, T., *Integration of Flow Injection Analysis and Zeptomole-Level Detection of the Fe(II)-o-Phenanthroline Complex*, *Anal. Sci.*, 15 (1999), 641-645.
- Scriven, L. E. and Sternling, C. S., *On cellular convection driven by surface tension gradients: effects of mean surface tension and surface viscosity*, *J. Fluid Mech.*, 19 (1964), 321-340.
- Sugii, Y., Nishio, S., Okuno, T. and Okamoto, K., *A highly accurate iterative PIV technique using gradient method*, *Meas. Sci. Technol.*, 11 (2000), 1666-1673.
- Sugii, Y. and Okamoto, K., *Quantitative Visualization of Micro-Tube Flow Using Micro-PIV*, *J. Visualization*, 7-1 (2004), 9-16.
- Tokeshi, M., Minagawa, T., Uchiyama, K., Hibara, A., Sato, K., Hisamoto, H. and Kitamori, T., *Continuous-Flow Chemical Processing on a Microchip by Combining Microunit Operations and a Multiphase Flow Network*, *Anal. Chem.*, 74 (2002), 1565-1571.
- Volpert, V. A., Pojman, J. A. and Texier-Picard, R., *Convection Induced by Composition Gradients in Miscible Systems*, *C. R. Mécanique*, 330 (2002), 353-358.
- Weigl, B. H. and Yager, P., *Microfluidics - Microfluidic diffusion-based separation and detection*, *Science*, 283 (1999), 346-347.

### *Author Profile*



Yasuhiko Sugii: He received his Ph.D. degree from Osaka Prefecture University in 2000. He worked in Kao Corporation from 1992 to 1995, and he was a post-doctoral fellow in Nuclear Engineering Research Laboratory, University of Tokyo from 2000 to 2002. He worked as a research associate in Nuclear Engineering Research Laboratory, University of Tokyo from 2002 to 2003 and University Illinois as a visiting scholar from 2003 to 2004. He works as a research associate in Department of Quantum Engineering and Systems Science, University of Tokyo since 2003. His research interests are in the image measurement of flow field, bio-fluid mechanics in blood flow and micro flow dynamics in MEMS and Micro TAS.



Koji Okamoto: He received his M.Sc.(Eng) in Nuclear Engineering in 1985 from University of Tokyo. He also received his Ph.D. in Nuclear Engineering in 1992 from University of Tokyo. He worked in Department of Nuclear Engineering, Texas A & M University as a visiting associate professor in 1994. He worked in Nuclear Engineering Research Laboratory, University of Tokyo as an associate professor from 1993 to 2004. He works as a professor in Department of Quantum Engineering and Systems Science, University of Tokyo since 2004. His research interests are Quantitative Visualization, PIV, Holographic PIV Flow Induced Vibration and Thermal-hydraulics in Nuclear Power Plant.



Akihito Hibara: He received his Ph.D. in applied chemistry from University of Tokyo in 2003. He worked in Department of Applied Chemistry, University of Tokyo as a research associate from 1999 to 2003. He works in Department of Applied Chemistry, University of Tokyo as a lecturer since 2003. His research interests are physical chemistry of liquids and liquid interfaces and chemophysical hydrodynamics of microfluidics.



Manabu Tokeshi: He is currently a group leader at the Kanagawa Academy of Science and Technology (KAST). He earned his Ph.D. degree in 1997 from Kyushu University. Following one year of postdoctoral study as a JSPS Postdoctoral Fellow at the University of Tokyo, he moved to the KAST where he is a research scientist in 1998-1999 and a sub-leader in 1999-2003. Tokeshi's current research projects are centered on the areas of miniaturized chemical analysis systems and ultra-high sensitive detection systems.



Takehiko Kitamori: He received his Ph.D. in chemical engineering from University of Tokyo in 1990. He worked in Hitachi, Ltd. from 1980 to 1990. He worked in Department of Applied Chemistry, University of Tokyo from 1990 to 1998 as a research associate, a lecturer, and an associate professor. He works in Department of Applied Chemistry, University of Tokyo as a professor since 1998. His research interests are applied laser spectroscopy and microchip chemistry and physics.